Optics Letters

Measuring refractive indices of a uniaxial crystal by structured light with non-uniform correlation

Rong Lin,[1,2] Mengyu Chen,[1] Yonglei Liu,[1] Hui Zhang,[1] Greg Gbur,[3,5] Yangjian Cai,[1,4,6] and Jiayi Yu[1,7]

[1]Shandong Provincial Engineering and Technical Center of Light Manipulations & Shandong Provincial Key Laboratory of Optics and Photonic Devices, School of Physics and Electronics, Shandong Normal University, Jinan 250014, China
[2]College of Physics and Electronics Engineering, Heze University, Heze 274015, China
[3]Department of Physics and Optical Science, University of North Carolina at Charlotte, Charlotte, North Carolina 28223, USA
[4]School of Physical Science and Technology, Soochow University, Suzhou 215006, China
[5]e-mail: gjgbur@uncc.edu
[6]e-mail: yangjiancai@suda.edu.cn
[7]e-mail: jiayiyu0528@sdnu.edu.cn

Received 4 March 2021; revised 2 April 2021; accepted 9 April 2021; posted 9 April 2021 (Doc. ID 424259); published 4 May 2021

We introduce an effective method for measuring the refractive indices of a uniaxial crystal based on the independent self-focusing property of non-uniformly correlated beams along the *x* and *y* directions. We demonstrate how the positions of the independent foci can be changed by adjusting coherence lengths to determine the characteristic coherence lengths of the beams in a uniaxial crystal, and how this information can be used to determine the refractive indices by relating the propagation characteristics of the beam in free space and in the crystal. Furthermore, it is demonstrated that, by choosing a high beam order, one can reduce the measuring error caused by CCD detection precision. These results present an example of how non-uniformly correlated beams can be used for applications in anisotropic materials. © 2021 Optical Society of America

https://doi.org/10.1364/OL.424259

It is well known that interesting and practical effects can be achieved by manipulating the amplitude, polarization, and phase of light beams. In recent years, the manipulation of spatial coherence has been recognized as another method to produce many peculiar physical phenomena [1,2]. Light beams with decreased spatial coherence are referred to as partially coherent beams (PCBs), and they often have advantages over their coherent counterparts [3]. PCBs are usually divided into conventional PCBs and non-conventional PCBs, according to whether or not the form of their degree of coherence (DOC) has a homogeneous Gaussian distribution [2]. Compared with conventional PCBs, non-conventional PCBs display much more extraordinary and versatile properties [2]. However, at the beginning of the 21st century, the difficulty of proving that a particular function was actually a mathematically valid correlation function limited investigations of non-conventional PCBs.

In 2007, Gori and Santarsiero derived sufficiency conditions for genuine correlation functions of scalar PCBs [4]. Their approach allows a wide variety of novel PCBs to be devised and generated that possess prescribed correlation properties. Since that discovery, researchers have studied the propagation properties of many new types of PCBs. It has been demonstrated that PCBs with prescribed correlation functions can exhibit behaviors such as self-focusing, self-shifting, self-splitting, as well as far fields with pre-established beam self-shaping [5–10]. It has also been verified that such beams maintain these unusual propagation characteristics in turbulent media [5,6,11,12]. Therefore, it is reasonable to believe that non-conventional PCBs can also exhibit peculiar propagation properties in other complex media.

Uniaxial anisotropic crystals have played an important role in designing wave plates, polarizing prisms, switches, and compensators due to their birefringent properties [13]. In 2001, Ciattnoi and his co-workers developed a simple vector theory for the paraxial propagation of beams in a uniaxial crystal [14]. Two years later, paraxial and non-paraxial conditions for light beams propagating along a direction perpendicular to the optical axis in a uniaxial crystal were studied [15]. The researchers found that, under the paraxial approximation, light beams with polarization parallel and perpendicular to the axis direction are independent, and they derived propagation expressions for vector light beams propagating perpendicular to the optical axis in a uniaxial crystal. Based on this, the propagation of various beams in a uniaxial crystal have been studied, and it has been confirmed that ordinary and extrordinary light beams will have different propagation velocities and the same propagation direction when light beams propagate perpendicular to the optical axis.

We can infer that the combination of the peculiar properties of non-conventional PCBs and a uniaxial crystal will lead to novel effects. Non-conventional PCBs will exhibit extraordinary propagation properties in a uniaxial crystal due to the interaction between the coherence properties and the anisotropy. So it is natural to wonder if we can take advantage of partial coherence to measure properties of a uniaxial crystal, such as refractive indices.

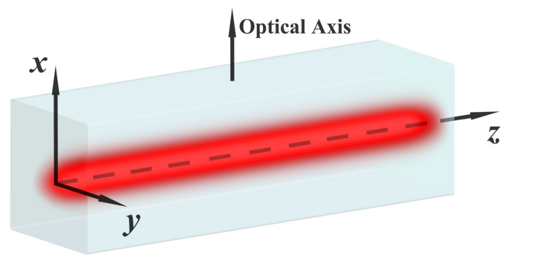

Fig. 1. Geometry of laser beam propagation in a uniaxial crystal orthogonal to the optical axis.

In this Letter, we focus on the intensity evolution of one class of non-conventional PCBs with a prescribed non-uniform correlation structure in a uniaxial crystal. The beams, rectangular Hermite non-uniformly correlated (RHNUC) beams, possess independent self-focusing properties in the x and y directions in the crystal. We demonstrate how to adjust the correlation structure of such beams to control the self-focusing property in a uniaxial crystal and then use the measured results to deduce the refractive indices of the crystal. These results are an example of how non-uniformly correlated PCBs can be used in applications in anisotropic media.

We start by discussing the paraxial propagation of laser beams in a uniaxial crystal in a direction orthogonal to the optical axis. The geometry is shown in Fig. 1, and with the optical axis of the crystal taken to coincide with the x axis, the dielectric tensor of a uniaxial crystal can be expressed as [13]

$$\varepsilon = \begin{bmatrix} n_e^2 & 0 & 0 \\ 0 & n_o^2 & 0 \\ 0 & 0 & n_o^2 \end{bmatrix}, \qquad \textbf{(1)}$$

where n_e and n_o denote the extraordinary and ordinary refractive indices of the crystal, respectively.

Under the paraxial approximation, the transverse components of the electric field propagating in a uniaxial crystal are shown in Eq. (9) in Ref. [15], and it can be readily concluded that the diffraction properties of the y component of the electric field are the same as a field propagating in an isotropic media, but the x component of the electric field undergoes a diffraction spreading asymmetry in the x and y directions. Therefore, in our work, we study laser beams with linear polarization in the x direction.

We will focus on using PCBs as a tool to measure the refractive indices of a uniaxial crystal. The paraxial propagation of the cross-spectral density (CSD) of PCBs in a direction perpendicular to the optical axis can be evaluated with the integral expression [16],

$$\begin{aligned} W(\boldsymbol{\rho}_1, \boldsymbol{\rho}_2) &= \tfrac{k^2 n_o^2}{4\pi^2 z^2} \iint W(\boldsymbol{r}_1, \boldsymbol{r}_2) \\ &\times \exp\left\{-\tfrac{ik}{2zn_e}\left[n_o^2(x_1-\rho_{x1})^2 + n_e^2(y_1-\rho_{y1})^2\right]\right\} \mathrm{d}^2\boldsymbol{r}_1 \\ &\times \exp\left\{\tfrac{ik}{2zn_e}\left[n_o^2(x_2-\rho_{x2})^2 + n_e^2(y_2-\rho_{y2})^2\right]\right\} \mathrm{d}^2\boldsymbol{r}_2, \end{aligned} \qquad \textbf{(2)}$$

where $W(\boldsymbol{r}_1, \boldsymbol{r}_2)$ and $W(\boldsymbol{\rho}_1, \boldsymbol{\rho}_2)$ denote the CSD of PCBs in the source and target plane, respectively. $\boldsymbol{r} = (x, y)$ and $\boldsymbol{\rho} = (\rho_x, \rho_y)$ are the position vectors at the input and target planes, and $k = 2\pi/\lambda$ is the free space wavenumber. We now focus specifically on the propagation of RHNUC beams in the crystal. The CSD of such beams in the source plane is expressed in Cartesian coordinates as [5]

$$W(\boldsymbol{r_1}, \boldsymbol{r_2}) = \exp\left(-\tfrac{r_1^2+r_2^2}{\omega_0^2}\right)\mu_x(x_1, x_2)\mu_y(y_1, y_2), \qquad \textbf{(3)}$$

where ω_0 is the beam width. The quantities μ_x and μ_y represent the DOCs of the RHNUC beam along the x and y directions, and can be expressed by the formula

$$\mu_\xi(\xi_1, \xi_2) = G_\xi \exp\left[-\frac{(\xi_1^2-\xi_2^2)^2}{\boldsymbol{\delta}_\xi^4}\right] H_{2m}\left(\frac{\xi_1^2-\xi_2^2}{\boldsymbol{\delta}_\xi^2}\right), \qquad \textbf{(4)}$$

where the subscript $\xi = x, y$ and $\boldsymbol{\delta}_\xi$ is the coherence length in the ξ direction. The quantity $G_\xi = 1/H_{2m}(0)$, where H_{2m} denotes the Hermite polynomial of order $2m$; m also denotes the beam order of the RHNUC beam.

When a RHNUC source is located in the plane $z = 0$ and radiates directly into a uniaxial crystal, we may calculate the CSD of RHNUC beams in the target plane of the crystal by substituting from Eqs. (3) and (4) into Eq. (2). However, there are higher-order terms in the CSD of RHNUC beams that make it difficult to calculate directly by integrating Eq. (2). Instead, we express the beam model in the form of a nonnegative definite kernel in two-dimensional integral form, as introduced in Ref. [5] [see Eq. (7)]. We then interchange the orders of the integrals and obtain the formula

$$W(\boldsymbol{\rho}_1, \boldsymbol{\rho}_2) = \int p(\boldsymbol{v})P(\boldsymbol{\rho}_1, \boldsymbol{\rho}_2, \boldsymbol{v}, z)\mathrm{d}^2\boldsymbol{v}, \qquad \textbf{(5)}$$

where $p(\boldsymbol{v})$, shown in Eq. (10) in Ref. [5], is the weighting function of the different beam modes that are contained in RHNUC beams and $P(\boldsymbol{\rho}_1, \boldsymbol{\rho}_2, \boldsymbol{v}, z)$ represents these different beam modes propagated to the target plane. This latter function can be written in a separated form,

$$\begin{aligned} &P_\xi(\rho_{1\xi}, \rho_{2\xi}, v_\xi, z_\xi) \\ &= \frac{k}{2\omega_\xi z_\xi} \exp\left[-\frac{ik}{2z_\xi}\left(\rho_{1\xi}^2 - \rho_{2\xi}^2\right)\right] \\ &\quad \times \exp\left[-\frac{ik^3}{4\omega_\xi^2 z_\xi^2}\left(v_\xi - \frac{1}{2z_\xi}\right)\left(\rho_{1\xi}^2 - \rho_{2\xi}^2\right)\right] \\ &\quad \times \exp\left[-\frac{k^2}{4\omega_\xi^2 z_\xi^2 \omega_0^2}\left(\rho_{1\xi}^2 + \rho_{2\xi}^2\right)\right]; \ (\xi = x, y), \end{aligned} \qquad \textbf{(6)}$$

with $\omega_\xi^2 = 1/\omega_0^4 + k^2[v_\xi - 1/(2z_\xi)]^2$ and

$$z_x = \frac{z_{cx}n_e}{n_0^2}; \quad z_y = \frac{z_{cy}}{n_e}, \qquad \textbf{(7)}$$

where $z_{c\xi}$ denotes the component of propagation distance in a uniaxial crystal in the ξ direction.

We obtain the propagated CSD of RHNUC beams in a uniaxial crystal by evaluating the integral of Eq. (5), and we obtain the spectral intensity of a RHNUC beam in the target plane from the usual definition,

$$S(\boldsymbol{\rho}, z) = W(\boldsymbol{\rho}, \boldsymbol{\rho}, z). \qquad \textbf{(8)}$$

With the above formulas, the propagation properties of RHNUC beams in a uniaxial crystal can be explored. Under the condition of $n_e = n_o = 1$, our formulas reduce to those of RHNUC beams propagating in free space, which we have

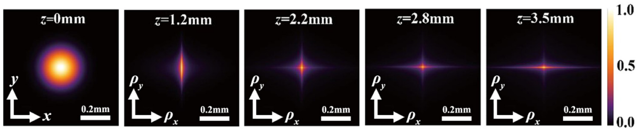

Fig. 2. The normalized intensity evolution of RHNUC beams at different propagation distances in a uniaxial crystal.

discussed in Ref. [5]. Let us define z_{fs} as the propagation distance in free space, and z_{fsx} and z_{fsy} are the x and y components of z_{fs}. Then, through Eq. (7), we can get the following expression relating the propagation distances in a uniaxial crystal and in free space,

$$\frac{z_{cx}}{z_{fsx}} = \frac{n_o^2}{n_e}; \qquad \frac{z_{cy}}{z_{fsy}} = n_e. \tag{9}$$

Therefore, if we can determine the propagation distances of RHNUC beams in a uniaxial crystal (z_{cx}; z_{cy}) and in free space (z_{fsx}; z_{fsy}) with the same initial beam parameters, we can calculate the extraordinary refractive index n_e and ordinary refractive index n_o of the crystal.

The next key question is, however, how do we determine the components of propagation distance in a uniaxial crystal and in free space under the same conditions? To answer this question, we first need to explore the propagation properties of RHNUC beams in a uniaxial crystal.

Let us explore the evolution of the spectral intensity of RHNUC beams propagating in a uniaxial crystal by numerical simulations. The beam parameters are set as $\lambda = 632.8$ nm, $\omega_0 = 0.15$ mm, $m = 1$, $\boldsymbol{\delta}_x = \boldsymbol{\delta}_y = 0.03$ mm; the refractive indices of the uniaxial crystal are taken as $n_o = 1.2$ and $n_e = 1.8 n_o$. The refractive indices here are arbitrary and chosen just to show the validity of the method.

Figure 2 shows the density plot of the normalized spectral intensity of RHNUC beams propagating in a uniaxial crystal at different propagation distances. From the evolution of the spectral intensity, we see that RHNUC beams display their self-focusing property in a uniaxial crystal, similar to the behavior in free space discussed in Ref. [5]. Furthermore, we can confirm that there is a quantitative difference in the crystal: RHNUC beams possess astigmatic focusing due to the effects of the uniaxial crystal. The extraordinary and ordinary refractive indices affect the positions of the foci, and, importantly, the same wavefront can be represented by the positions of the foci. Thus, we can deduce the extraordinary and ordinary refractive indices from these focal positions.

In order to show the position of the focus clearly, we plot the normalized intensity on-axis of RHNUC beams on propagation in a uniaxial crystal in Fig. 3. First, let us consider the total intensity (S_t, black line; $S_t = S_x \times S_y$); we observe there are two peaks of the normalized intensity of such beams on propagation, which means RHNUC beams have been focused astigmatically, as we can see from Fig. 2 or the red dashed–dotted line (S_x, the normalized component intensity in x direction) and blue dotted line (S_y, the normalized component intensity in y direction) in Fig. 3; these two foci are from the foci in x and y directions, respectively. Therefore, we can get the components of propagation distance z_{cx} and z_{cy} in a uniaxial crystal from Fig. 3, $z_{cx} = 1.135$ mm and $z_{cy} = 3.684$ mm. If we want to deduce the refractive indices of the uniaxial crystal, we also need the value of the corresponding propagation distance z_{fs} in free

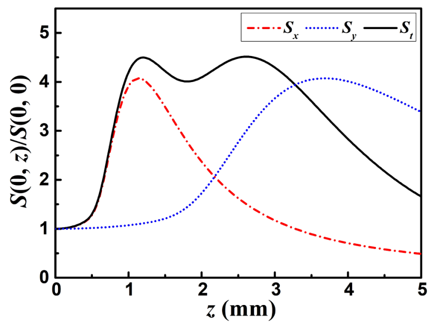

Fig. 3. Normalized intensity on-axis of RHNUC beams on propagation in a uniaxial crystal.

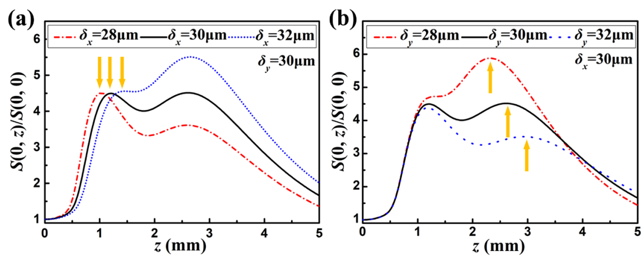

Fig. 4. Normalized intensity on-axis of RHNUC beams on propagation in a uniaxial crystal for different coherence lengths.

space. Fortunately, we can get it by using Eqs. (5)–(8) and setting $n_o = n_e = 1$; from this, we get $z_{fsx} = z_{fsy} = z_{fs} = 1.705$ mm readily.

We, therefore, can determine that the extraordinary and ordinary refractive indices of the crystal are $n_e = 2.16$ and $n_o = 1.2$, using the values of z_{cx}, z_{cy}, z_{fsx}, and z_{fsy} and Eq. (9). Here, we need to make a statement, in the above context, that the value of n_e is arbitrary, so we write it as $n_e = 1.8 n_o$. And we calculated here $n_e = 2.16$ ($n_e = 1.8 n_o = 2.16$), which shows the correctness of our method.

The method as described so far is not convenient for experimental measurements because the components of propagation distance z_{cx} and z_{cy} are typically inside the crystal. We now refine our method for experimental convenience.

Let us continue to explore the spectral intensity evolution of RHNUC beams in a uniaxial crystal. Figure 4 shows the normalized intensity on-axis of RHNUC beams on propagation in a uniaxial crystal for different components of coherence lengths $\boldsymbol{\delta}_x$ and $\boldsymbol{\delta}_y$. We can confirm from this figure that the positions of the two peaks can be moved by adjusting the coherence lengths. For example, adjusting $\boldsymbol{\delta}_x$ ($\boldsymbol{\delta}_y$) can move the left (right) peak, and increasing the value of either coherence length can move the corresponding peaks to the right side. Therefore, through this extraordinary propagation property of RHNUC beams, we can "shift" the components of propagation distance z_{cx} and z_{cy} to the output surface plane of the crystal.

In a practical case, when we take a uniaxial crystal with unknown refractive indices, what we can measure directly is the crystal length. Let us assume that a uniaxial crystal of refractive indices to be measured is 3 mm long. We plot the normalized on-axis intensity of RHNUC beams propagating in the uniaxial crystal in Fig. 5(a). The black dashed line represents the output surface of the crystal. In order to better show the trend of the normalized intensity on-axis, we extended the propagation

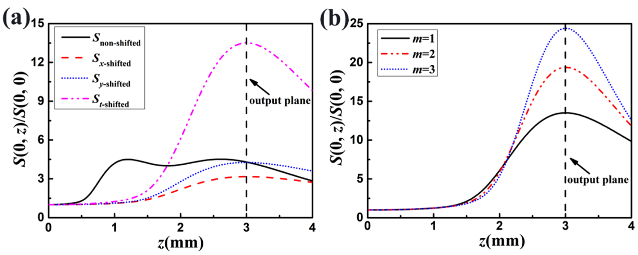

Fig. 5. Shifted normalized intensity on-axis of RHNUC beams on propagation in a uniaxial crystal.

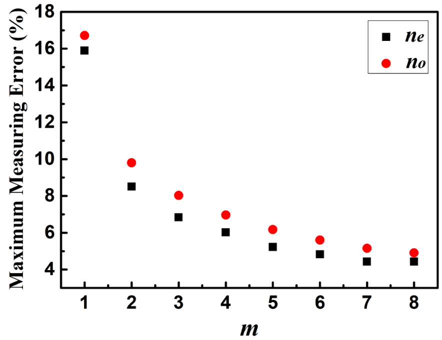

Fig. 6. The maximum measuring error of n_e and n_o with different beam order.

distance appropriately in Fig. 5(a). The black solid line represents the normalized intensity on-axis before the "shifting" of RHNUC beams with coherence lengths $\boldsymbol{\delta}_x = \boldsymbol{\delta}_y = 0.03$ mm. Its two peaks appear inside the crystal, making it hard to measure the exact component of propagation distance z_{cx} and z_{cy}. The pink dashed–dotted line represents the normalized intensity of RHNUC beams on-axis after adjusting the coherence lengths. The red dashed line and blue dotted line represent the normalized intensity components in x and y directions, respectively. Coherence lengths $\boldsymbol{\delta}_x$ and $\boldsymbol{\delta}_y$ are adjusted to move the two component peaks to $z = 3$ mm, i.e., the output surface of the crystal. The intensity on-axis we measure now is at its maximum. Let us define the coherence lengths at this time as "characteristic coherence lengths" (CCLs) ($\boldsymbol{\delta}_{xc}$; $\boldsymbol{\delta}_{yc}$) of such beams. According to the determined CCL ($\boldsymbol{\delta}_{xc}$; $\boldsymbol{\delta}_{yc}$) and Eqs. (5)–(8), and setting $n_o = n_e = 1$, we can get the corresponding value of the propagation distances in free space z_{fsx} and z_{fsy}. So we can get the value of the extraordinary and ordinary refractive indices of the crystal based on the values of z_{cx}, z_{cy}, z_{fsx}, and z_{fsy} and the relational expression Eq. (9).

Let us concisely summarize the measurement process. First, a crystal with unknown refractive index is placed with one of the surfaces of the crystal in the source plane. Second, a CCD is placed to monitor the on-axis intensity of the output plane. Third, the coherence length components $\boldsymbol{\delta}_x$ and $\boldsymbol{\delta}_y$ of RHNUC beams are adjusted until the CCD detects the maximum intensity, providing CCL $\boldsymbol{\delta}_x$ and $\boldsymbol{\delta}_y$. The propagation distance components z_{fsx} and z_{fsy} of such beams in free space under the CCL are calculated. Finally, from the values of z_{fsx}, z_{fsy}, z_{cx}, and z_{cy} (i.e., length of crystal), we can get the extraordinary and ordinary refractive indices of the crystal to be measured.

One practical concern is the measurement accuracy of the CCD: because the intensity peaks are of finite width, there will naturally be uncertainty in the measurement of their positions. Fortunately, it has been discussed in Ref. [5] that a RHNUC beam with large beam order has a more dramatic self-focusing property, producing a narrower intensity peak. This property can reduce the measuring error caused by CCD detection precision. Figure 5(b) shows the shifted normalized intensity on-axis of RHNUC beams on propagation in a uniaxial crystal with different beam orders. One confirms that the peak becomes narrower with increasing beam order, which can reduce the measuring error by the CCD. Assuming the CCD cannot resolve intensity greater than 99% of the maximum intensity, we determine the dependence of the measuring error of the maximum with the beam order in Fig. 6. One confirms that the maximum measurement error decreases with the increase of the beam order, and the extraordinary refractive index n_e measurement error is smaller than the ordinary refractive index n_o; because the latter is measured based on the former [see Eq. (9)], the measurement error of n_e will be counted into that of n_o.

In conclusion, we have studied the intensity evolution of RHNUC beams propagating in a uniaxial crystal, and we demonstrated how the refractive indices of the crystal can be measured by coherence techniques. This technique shows the potential of non-uniformly correlated beams in applications involving the propagation of light through anisotropic media.

Funding. National Key Research and Development Program of China (2019YFA0705000); National Natural Science Foundation of China (11525418, 11904087, 11947240, 12004218, 1750201); China Postdoctoral Science Foundation (2020M680093); Natural Science Foundation of Shandong Province (ZR2020QA067); Local Science and Technology Development Project of the Central Government (YDZX20203700001766); Innovation Group of Jinan (2018GXRC010).

Disclosures. The authors declare no conflicts of interest.

Data Availability. All data that support the findings of this study are included within the article.

REFERENCES

1. O. Korotkova and G. Gbur, Prog. Opt. **65**, 43 (2020).
2. Y. Cai, Y. Chen, J. Yu, X. Liu, and L. Liu, Prog. Opt. **62**, 157 (2017).
3. G. Gbur, J. Opt. Soc. Am. A **31**, 2038 (2014).
4. F. Gori and M. Santarsiero, Opt. Lett. **32**, 3531 (2007).
5. J. Yu, Y. Cai, and G. Gbur, Opt. Express **26**, 27894 (2018).
6. X. Zhao, L. Zhang, R. Lin, S. Lin, X. Zhu, Y. Cai, and J. Yu, Chin. Phys. Lett. **37**, 124202 (2020).
7. Y. Chen, J. Gu, F. Wang, and Y. Cai, Phys. Rev. A **91**, 013823 (2015).
8. Y. Chen, S. A. Ponomarenko, and Y. Cai, Appl. Phys. Lett. **109**, 061107 (2016).
9. X. Zhu, J. Yu, Y. Chen, F. Wang, O. Korotkova, and Y. Cai, Appl. Phys. Lett. **117**, 121102 (2020).
10. S. Sahin and O. Korotkova, Opt. Lett. **37**, 2970 (2012).
11. J. Yu, X. Zhu, F. Wang, D. Wei, G. Gbur, and Y. Cai, Opt. Lett. **44**, 4371 (2019).
12. Y. Yuan, X. Liu, F. Wang, Y. Chen, Y. Cai, J. Qu, and H. T. Eyyuboğlu, Opt. Commun. **305**, 57 (2013).
13. M. Born and E. Wolf, *Principles of Optics* (Cambridge University, 1999).
14. A. Ciattoni, B. Crosignani, and P. Di Porto, J. Opt. Soc. Am. A **18**, 1656 (2001).
15. A. Ciattoni and C. Palma, J. Opt. Soc. Am. A **20**, 2163 (2003).
16. D. Liu and Z. Zhou, J. Opt. Soc. Am. A **26**, 924 (2009).